Supporting Information

Reconstitution and Functional Analysis of a Full-Length Hepatitis C Virus NS5B Polymerase on a Supported Lipid Bilayer

Nam-Joon Cho[1,2,*#], Edward Pham[2,3#], Rachel J. Hagey[3], Vincent J. Lévêque[4], Han Ma[4], Klaus Klumpp[4], and Jeffrey S. Glenn[2,3,5,+]

[1]Department of Chemical Engineering, Stanford University, Palo Alto, California;
[2]Department of Medicine, Division of Gastroenterology and Hepatology, Stanford University School of Medicine, Palo Alto, California;
[3]Department of Microbiology and Immunology, Stanford University School of Medicine, Palo Alto, California;
[4]Virology Discovery, Hoffmann-La Roche Inc., Nutley, New Jersey;
[5]Veterans Administration Medical Center, Palo Alto, California

* current address: Nanyang Technological University, Singapore

#These authors contributed equally to this work.

+ To whom correspondence should be addressed:

Dr. Jeffrey S. Glenn, Department of Medicine, Division of Gastroenterology and Hepatology, Stanford University School of Medicine, Stanford University, CCSR 3115A, 269 Campus Drive, Stanford, CA, 94305-5171; Tel:(650) 725-3373; Fax:(650) 723-3032; Email: jeffrey.glenn@stanford.edu

Supplementary Materials and Methods.

Supporting Figure 1. Denaturing Polyacrylamide Gel of Recombinant Proteins Used in this Study.

Supporting Figure 2. Proposed Model for NS5B-FL in solution.

Supporting Figure 3. SLB Platform on the Quartz Crystal Microbalance with Dissipation Monitoring (QCM-D) Nanomass Sensor.

Supporting Figure 4. Membrane Association of Recombinant HCV NS5B-FL and its C-terminal deletion mutants.

Supporting Figure 5. QCM-D Kinetics of NS5B C-Terminal Peptide Binding to SLB Platform.

Supporting Figure 6. Full length NS3 alone does not associate with membranes.

Supporting Figure 7. Full Kinetic Traces for Step-by-Step Assembly and RNA-Dependent RNA Polymerase (RdRp) Activity of the Membrane-Associated HCV Replicase Complex.

Supporting Figure 8. No polymerase activity is observed when fewer than all four native NTP species are added.

Supporting Figure 9. NS5AΔ32 Directly Binds to NS5B-FL.

Supporting Figure 10. Northern blot analysis of QCM products.

Supporting Figure 11. Chemical structures of non-nucleoside HCV NS5B inhibitors HCV-796 and VX-222.

Supporting Table 1. Summary of Kinetic Values.

Supporting Table 2. QCM-D Measurement Data of Immobilized NS5B-FL Protein and Enzyme Kinetics.

Materials and Methods

Protein purifications

Recombinant full-length HCV NS3 proteins from Con1 or BK strains (NS3-FL-Con1 and NS3-FL-BK) were expressed in E.coli BL21(DE3) cells. Lysates were prepared by suspension of cell pellets in NS3-FL disruption buffer (50 mM Tris-HCl pH 7.8, 20% glycerol, 500 mM NaCl, 0.05% maltopyranoside, 10 mM β-mercaptoethanol (BME), 10 mM imidazole), 10 U/ml benzonase and one complete protease inhibitor tablet (Roche) per 50 ml disruption buffer. Suspensions were disrupted by micro fluidization at 14K psi and 120 psi respectively, spun for 30 min at 14, 000 rpm or 18, 000 RCF respectively to remove debris. Supernatants were filtered using 0.45 micron filters and loaded onto a Ni-NTA (Qiagen) or immobilized metal affinity chromatography (GE healthcare) columns respectively. Columns were pre-equilibrated with buffer A (disruption buffer that did not contain protease inhibitors or nuclease). Columns were washed with buffer A until baseline was re-established and eluted with a 10 column volumes (CV) gradient 0-100% buffer A to buffer B (buffer A + 250 mM imidazole, pH 7.8). Gradient peaks were collected and dialyzed in 4x volume of buffer C (50 mM Tris, pH 7.8 plus 20% glycerol, 0.05% maltopyranoside/ dodecyl maltoside, 2 mM DTT) for 40 h. Dialyzed solutions were centrifuged and supernatant loaded onto a heparin-sepharose HP column (GE healthcare) pre-equilibrated in 5-10 CV buffer D (buffer C plus 0.1M NaCl). Columns were washed with buffer D and protein eluted in 6 CV using a gradient from 0.1 M to 0.4 M NaCl in buffer D. Peak fractions were pooled, NaCl adjusted to a final concentration of 0.5 M and stored at -80°C.

NS3-helicase domain from HCV BK strain was purified from E.coli cell pellets that were resuspended in lysis buffer (50 mM Tris-HCl, pH 8.0, 500 mM NaCl, 1 mM DTT, 20 mM imidazole) and protease inhibitor cocktail (Roche Diagnostic) with stirring for 1 h followed by passage through a micro fluidizer and centrifugation at 186,000×g for 45 min. Supernatant was filtered and loaded onto two tandem 5 mL HisTrap™ HP columns (GE healthcare) equilibrated with buffer A (lysis buffer without protease inhibitors). Proteins were eluted with a linear gradient to 1 M imidazole in buffer A, peak fractions were pooled and further purified by gel filtration on a Superdex 200 26/60 column (GE healthcare), equilibrated in buffer A.

NS3 protease domain protein NS3-Protease-BK was prepared from E.coli cell pellets by lysis in NS3-PD disruption buffer (50mM HEPES, pH 8.0, 0.3M NaCl, 10% Glycerol, 0.1% octyl glucoside, 5 mM BME, 5 mM imidazole), 1X complete EDTA-free protease inhibitor (Roche) and10 U/ml benzonase, followed by homogenization, micro fluidization, centrifugation and filtration as described above for full-length NS3 protein. The filtrate was run through an IMAC column pre-equilibrated in IMAC buffer A (disruption buffer) and eluted in 25 column volumes of a gradient of IMAC buffer B (buffer A + 300 mM imidazole) from 0-100%. Peak fractions were pooled and concentrated to 2 ml and then loaded onto a superdex 75 column equilibrated in buffer A. Peak fractions were pooled, concentrated to ~1-2 mg/ml using an Amicon ultra centrifugal filtration device (10 kDa MWCO).

NS5A protein HCV His6-NS5A BK (33-447) was purified from E.coli cell pellets that were resuspended in NS5A lysis buffer (50 mM Tris-HCl, pH 8.0, 500 mM NaCl, 1 mM

DTT, 20 mM imidazole) and protease inhibitor cocktail (Roche Diagnostic) with stirring for 1 h followed by passage through a micro fluidizer and centrifugation at 186,000×g for 45 min. The supernatant was filtered and loaded onto three tandem 5 mL HiTrap™ heparin columns also equilibrated with lysis buffer. Protein was eluted using a linear gradient of 50 mM to 1 M NaCl. This chromatography was repeated to optimize protein purity to homogeneity. The protein was dialyzed with storage buffer (50mM Tris-HCl, pH 8.0, 150 mM NaCl, 5 mM DTT, 10% glycerol).

NS5A N-terminal domain was purified from E.coli cell pellets that were resuspended in NS5A lysis buffer (25 mM Tris, pH 8.0, 50 mM NaCl, 10 % glycerol, 0.1 % igepal CA-630 (Sigma), 20 mM imidazole, 1 X complete EDTA-free protease inhibitors (Roche) and 10 U/ml benzonase) with stirring for 1 h followed by passage through a micro fluidizer and filtration using 0.45 micron filters. The filtrate was run through a Ni-NTA column pre-equilibrated with buffer A (25 mM Tris-HCL, pH 8.0, 400 mM NaCl, 10 % glycerol, 0.1 % igepal CA-630 (Sigma) and 20 mM imidazole), and eluted with 0-100% gradient of buffer A to buffer B (buffer A + 200 mM imidazole). Peak fractions were desalted by gel filtration and further purified using a resource Q column pre-equilibrated with buffer A2 (25 mM Tris-HCL, pH 8.0, 50 mM NaCl and 10% glycerol) and eluted with buffer B2 (A2 + 1 M NaCl). Peak fractions were concentrated to ~ 2.5 ml and loaded onto an SEC column pre-equilibrated with SEC buffer (25 mM HEPES, pH 8.0, 250 mM NaCl and 10% glycerol). Peak fraction were pooled and concentrated before storage.

Generation of RdRp template and assay conditions in solution

A 377 nucleotide RNA template (the 3' terminus of the viral negative strand RNA, termed "cIRES") was generated as described in Klumpp et al (*J Biol Chem* 281(7):3793-3799). Briefly, 377 nucleotides cIRES RNA, from the 3´-end of HCV (-)-strand RNA, was synthesized in vitro using a T7 RNA polymerase transcription kit (Ambion, Inc.) and purified either by phenol-chloroform extraction or using the Qiagen RNeasy maxi kit, with similar results. In vitro HCV polymerase reactions contained 10 µg/ml cIRES RNA template, 50 nM polymerase protein, 1 µM tritiated UTP or CTP (1–5 µCi), 1 µM ATP, 1 µM CTP, 1 µM GTP, 40 mM Tris-HCl pH 8.0, 4 mM dithiothreitol, and 4 mM $MgCl_2$ and were performed as described in Klumpp et al (*J Biol Chem* 281(7):3793-3799).

SLB experiments

For supported lipid bilayer experiments, lipid bilayers were formed on the solid support using 10 mM Tris buffer [pH 7.5] with 150 mM NaCl. After bilayer formation, a buffer-exchange was performed and 40 mM Tris-HCl buffer [pH 8.0] with 50 mM NaCl, 4 mM $MgCl_2$ and 4 mM DTT ("reaction buffer") was introduced and used as the buffer for all protein binding and activity measurements. Proteins and cIRES RNA template were introduced into the QCM chamber at a final concentration of 87 µg/ml and 50 µg/ml, respectively. Protein and nucleotide dilutions were carried out in reaction buffer and the final nucleotide concentrations for the replicase measurements were 500 µM per nucleotide (ATP, UTP, GTP and CTP). For inhibition studies involving inhibitor, 500 µM of inhibitor was added together with 500 µM of each nucleotide (ATP, UTP, GTP and CTP).

Supporting Figure 1. Denaturing Polyacrylamide Gel of Recombinant Proteins Used in this Study. One microgram of each protein was loaded onto a 4-12% Bis-Tris gel and run at 150V for 80 minutes. Gel was stained using SimplyBlue Safe Stain (Life Technologies). Loading was as follows: (L) BenchMark™ ladder, (1) NS5B-FL, (2) NS5B-Δ21, (3) NS5A-Δ32, (4) NS3-FL, (5) NS3 Protease domain, (6) NS3 Helicase domain.

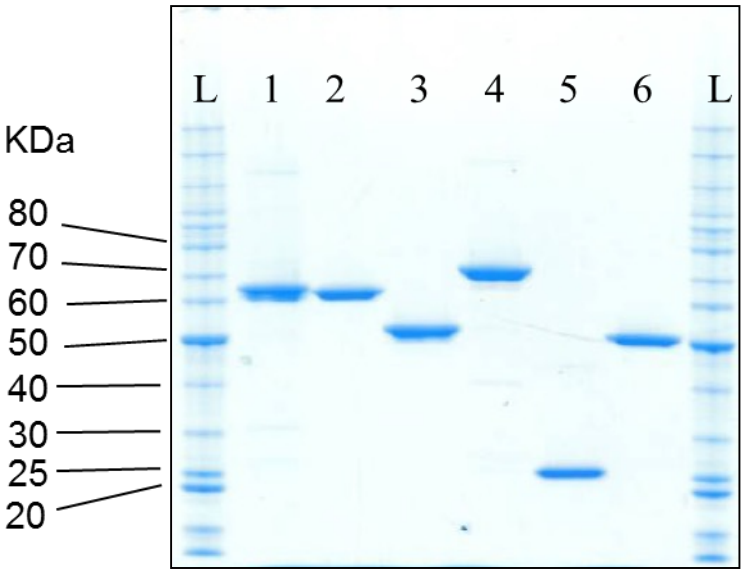

Supporting Figure 2. Schematic models of NS5B-FL protein in solution and associated with bilayer membrane.

The models are based on the NS5b-Δ21 crystal structure 1C2P.[1] **A**, NS5b-Δ21 crystal structure with the active site residues colored in red. **B**,model of the membrane-bound NS5B-FL protein. The model of the 28-mer C-terminal sequence that is missing in the 1C2P crystal structure was constructed via Pymol (Schrödinger LLC), as an extension from Ser-563 (564-LSRARPRWFM LCLLLLSVGV GIYLLPNR, transmembrane domain underligned and in agreement with TMHMM ((http://www.cbs.dtu.dk/services/TMHMM/)). Using an overall extended conformation, the resulting structure was energy-minimized using BABEL (http://www.ncbi.nlm.nih.gov/pubmed/?term=21982300). The C-terminal end of NS5B-FL is of sufficient length and has appropriate properties to form a transmembrane domain (colored in yellow), and to bring the polymerase protein into close contact with the membrane. **C**, model of NS5B-FL in solution. In solution, the C-terminal domain (colored in yellow) may fold back into the active site and act as a polymerase inhibitory domain. The model was built using Pymol, taking into account hydrophobic and electrostatic interactions, H-bonding and secondary structure constraints. The C-terminus was modeled as a helix-turn-helix, with a helical propensity towards 3_{10} helices. It has sufficient length to reach and block the opening to the active site, while the hydrophobic residues in the transmembrane domain have reduced solvent exposure. Energy minimizations, but no large-scale molecular dynamics simulations were performed.

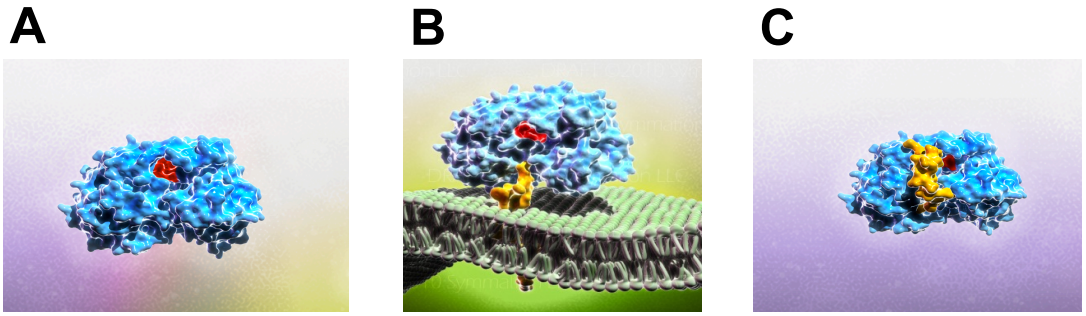

Supporting Figure 3. SLB Platform on the Quartz Crystal Microbalance with Dissipation Monitoring (QCM-D) Nanomass Sensor.

A) Overview of the QCM-D measurement principle. The QCM-D technique permits real-time monitoring of mass adsorption onto a quartz crystal substrate [2]. The piezoelectric quartz crystal is positioned between two electrodes, and oscillates when an AC voltage is applied across it. When additional mass (e.g., lipid vesicles) adsorbs onto the substrate, the crystal's resonance frequency of oscillation decreases. The frequency change, Δf, is proportional to the mass of the adsorbed material. To describe the adsorbed material's viscoelastic properties, the circuit can be opened, permitting the crystal's oscillation to decay exponentially. The energy loss per stored energy during one oscillation cycle is referred to as the energy dissipation, D, which is proportional to 1/τ, where τ is the decay time constant. Films with large viscous loss will display larger ΔD than more rigid films because the ratio between energy loss and stored energy will be larger. **B) Intact vesicle platform.** On surfaces that include titanium oxide and gold, lipid vesicles adsorb but do not rupture due to insufficient adhesion energy. The result is a full monolayer of adsorbed, unruptured vesicles. **C) Supported lipid bilayer (SLB) platform**. On a silicon oxide surface, the adhesion energy can be sufficient to result in the rupture of lipid vesicles and thus a spontaneous formation of a lipid bilayer from vesicles (SLB platform self-assembly). **D) QCM-D kinetic trace for SLB platform self-assembly.** The characteristic SLB formation signature is a two-step kinetic process. Lipid vesicles first adsorb and remain intact on silicon oxide, resulting in a decrease in frequency (Δf), consistent with addition of mass to the surface and an increase in dissipation (ΔD). After reaching a critical surface coverage of lipid vesicles, the combination of vesicle-vesicle and vesicle-substrate interactions promotes the rupture of lipid vesicles and the formation of a lipid bilayer. This lipid bilayer assembly process is characterized by an increase in Δf to ~24 Hz (consistent with the loss of mass as compared to the vesicle surface) and a decrease in ΔD. Note that the critical surface coverage necessary for vesicle rupture and SLB formation depends on a number of experimental parameters, including vesicle size, lipid composition, ionic strength, osmotic pressure, pH, and temperature.[2-7] As such, the Δf and ΔD values corresponding to the critical surface coverage can vary. Further, in cases where there are very strong vesicle-surface interactions, vesicle rupture and SLB formation can be accelerated and proceed through apparent one-step kinetics.

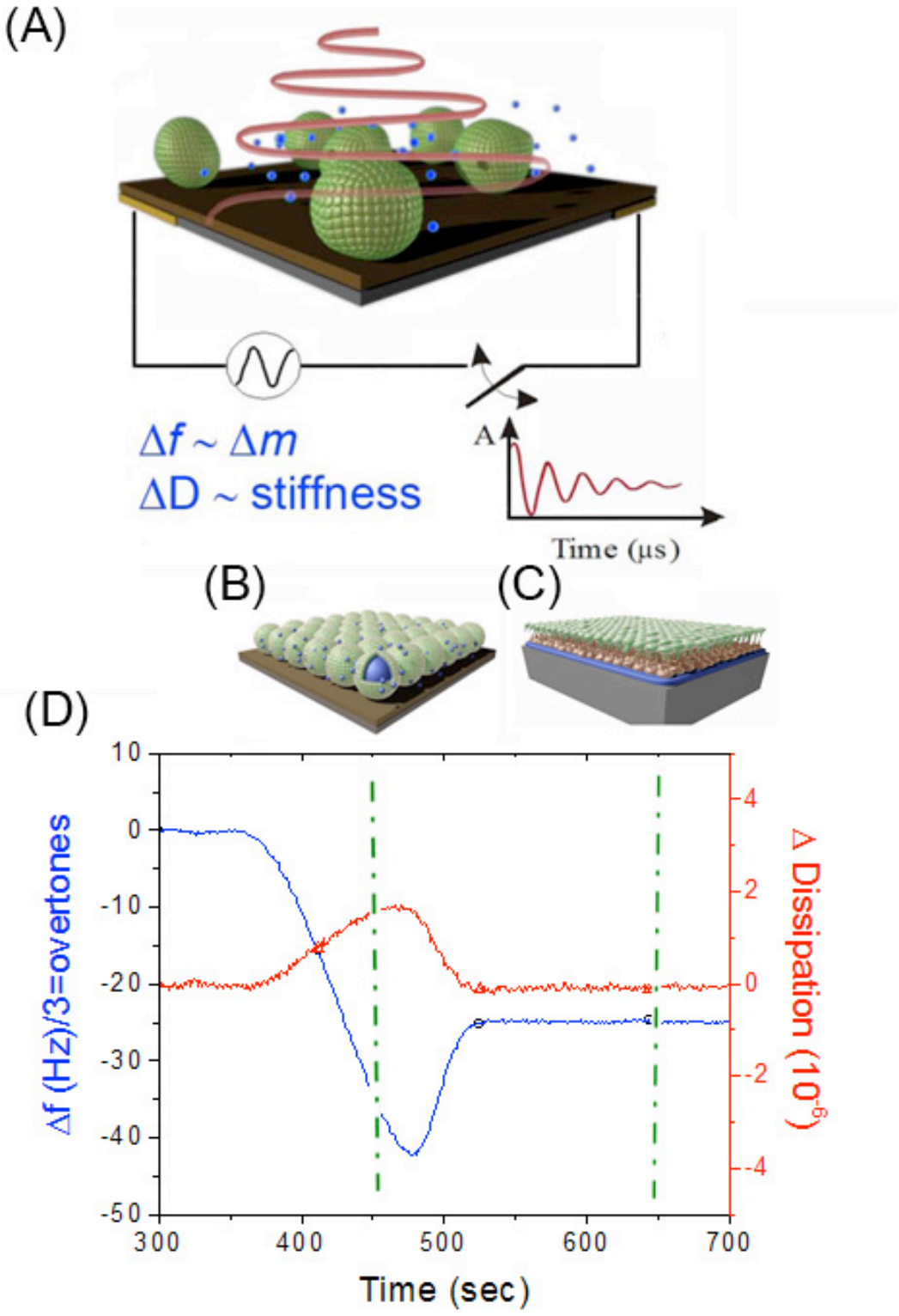
(A)
Δf ~ Δm
ΔD ~ stiffness
A
Time (μs)
(B)
(C)
(D)
Δf (Hz)/3=overtones
Δ Dissipation (10⁻⁶)
Time (sec)
10
0
-10
-20
-30
-40
-50
4
2
0
-2
-4
300
400
500
600
700

238

239

Supporting Figure 4. Membrane Association of Recombinant HCV NS5B-FL and its C-terminal deletion mutants. A) Membrane association of NS5B-FL-c-His protein (this full length NS5b protein carries an additional His-tag label on the C-terminus). The protein is added at the 30min time point (arrow), resulting in a large increase in dissipation (red curve) and a reduction in frequency (blue curve), consistent with the addition of protein mass to the bilayer membrane. **B)** Addition (arrow) of the truncated protein lacking the C-terminal 21 amino acids, but carrying a N-terminal His-tag (NS5BΔ21-n-His), or **C)** addition (arrow) of the truncated protein lacking the C-terminal 21 amino acids, but carrying a C-terminal His-tag, (NS5BΔ21-c-His) did not lead to changes in frequency, consistent with the lack of membrane binding of the truncated NS5b proteins.

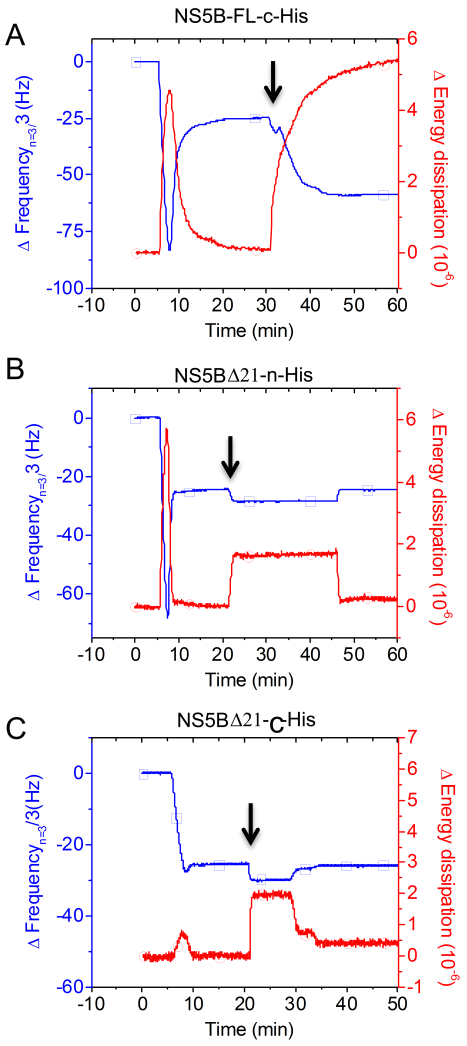

Supporting Figure 5. QCM-D Kinetics of NS5B C-Terminal Peptide Binding to the immobilized lipid bilayer. The interaction of a 21 amino acid long peptide corresponding to the NS5B C-terminus with the SLB platform was investigated by QCM-D monitoring of resonance frequency (red) and energy dissipation (blue). **A)** At 6 μM NS5B C-terminal peptide concentration, peptide binding to the lipid bilayer indicated by a reduction in frequency (blue). The kinetic behavior suggested membrane penetration, as indicated by the kink in signal response (highlighted by circles) that is indicative of peptide rearrangement at the membrane interface, an initial increase in mass from the addition of peptide, followed by a loss of mass from the displacement of lipid from the surface. The compensatory loss of mass after peptide addition differentiates membrane penetration through the lipid bilayer from simple adhesive peptide binding to the bilayer surface. **B)** At 12 μM NS5B C-terminal peptide concentration, the initial frequency change was doubled (consistent with the addition of double mass). Together, the QCM-D responses demonstrate that the NS5b C-terminal peptide shows concentration-dependent binding kinetics indicative of membrane penetration.[8]

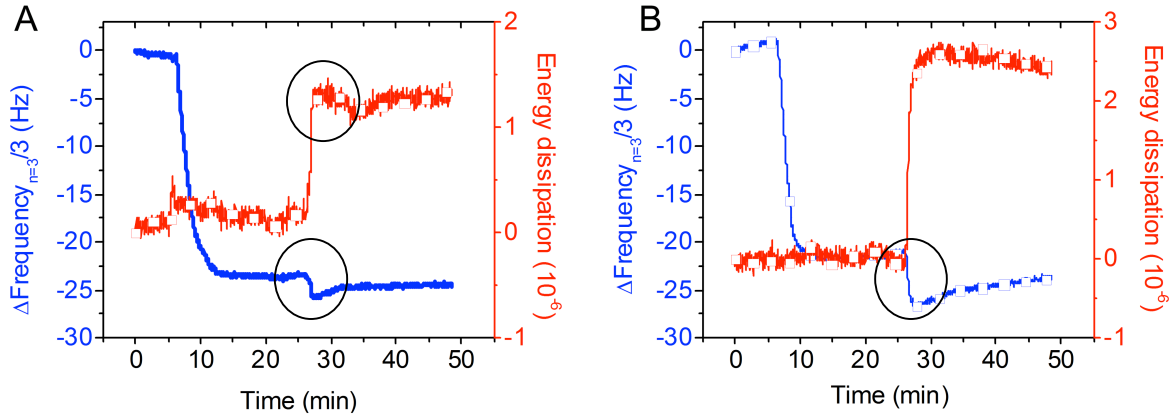

Supporting Figure 6. Full length NS3 protein alone does not associate with lipid bilayer membranes. A) Addition (arrow) of NS3-FL-BK (full length NS3 from HCV BK strain) or **B)** addition (arrow) of NS3-FL-CON (from Con1 strain) protein to the immobilized lipid bilayer does not result in significant frequency or dissipation changes, indicating lack of binding.

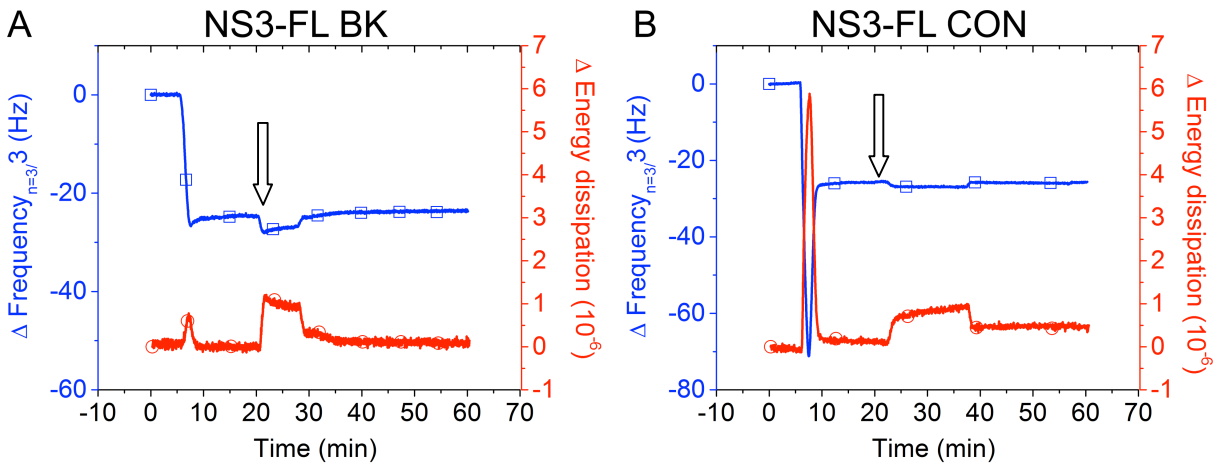

Supporting Figure 7. Full Kinetic Traces for Step-by-Step Assembly and RNA-Dependent, RNA Polymerase (RdRp) Activity of the Membrane-Associated HCV Replicase Complex. Individual replicase complex components were sequentially added to the sensing chamber and buffer exchanges performed as indicated by arrows in the Figure panels: **A)** SLB only, formation of an immobilized bilayer membrane; **B)** SLB + NS5B-FL, binding of NS5b protein to the membrane bilayer; **C)** RNA polymerase activity of NS5b; after formation of the NS5b containing bilayer membrane, a buffer exchange was performed into polymerase buffer (leading to an slight increase in frequency) and then cIRES RNA added, which bound to the immobilized NS5b, as indicated by the frequency decrease; when ribonucleoside triphosphates (rNTPs) were added, a slow, but continuous decrease in frequency was observed, consistent with continuous addition of nucleosides to the immobilized polymerase-cIRES RNA complex (polymerase activity) **D)** RNA polymerase activity of the NS5b-NS3 complex; NS3 was added to immobilized NS5b and binding observed by reduced frequency. Then cIRES RNA and NTPs were added. **E)** RNA polymerase activity in the presence of NS5a; NS5a was added to immobilized NS5b and binding observed by reduced frequency. Then cIRES RNA and NTPs were added. **F)** Binding of RNA prior to NS5a; in a changed sequence of complex formation, cIRES RNA was added to immobilized NS5b first. Then NS5a and NTPs were added. **G)** Polymerase reaction as (C), except that the chain-terminating inhibitor, 3′-dCTP, was added after 500min to stop the polymerase reaction. RdRp activity was calculated based on the total increase of mass associated with rNTP polymerization per bound NS5B per minute of polymerization, enabling determination of the apparent k_{cat} and total amounts of RNA synthesized. Main panels: representative QCM-D resonance frequency tracings; inset panels: magnified view of corresponding QCM-D tracing for polymerase kinetics upon rNTP addition.

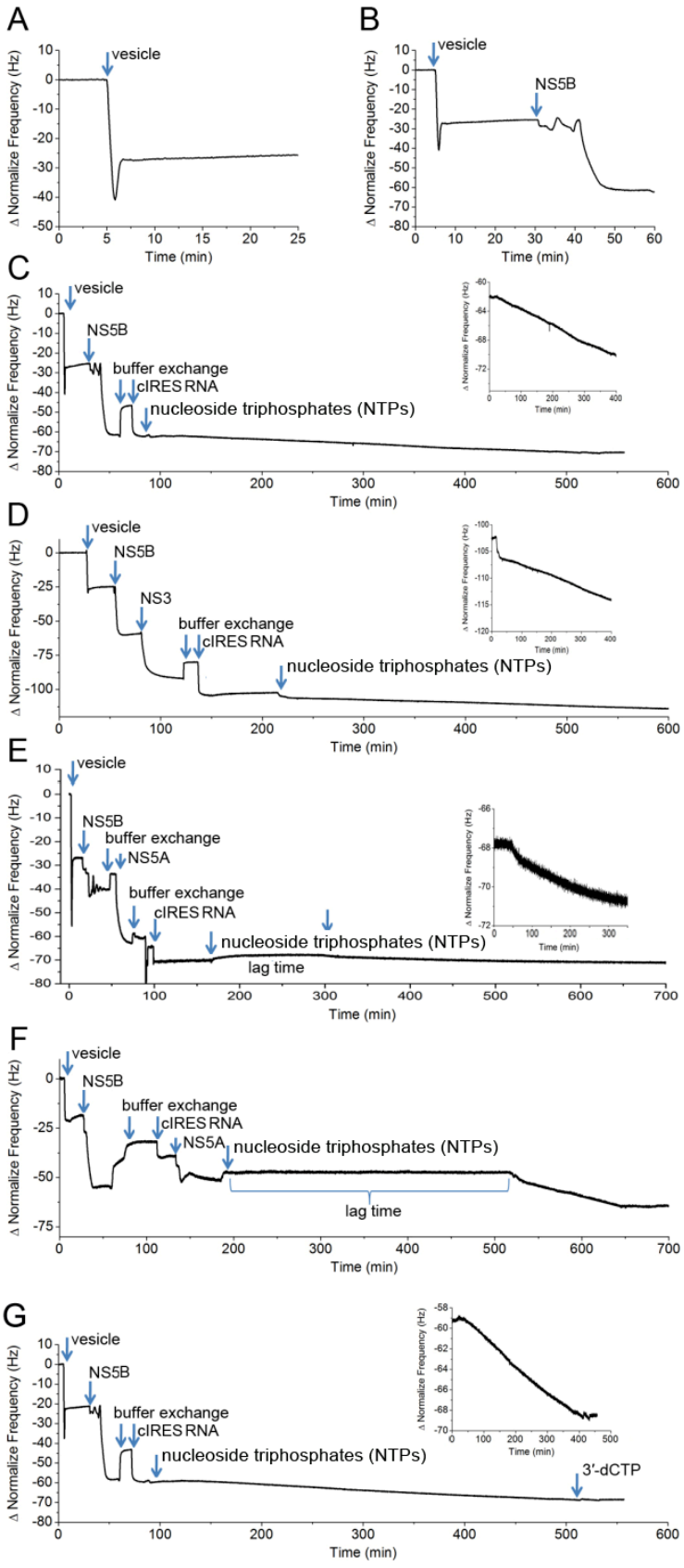
A
vesicle
Δ Normalize Frequency (Hz)
Time (min)
B
vesicle
NS5B
Δ Normalize Frequency (Hz)
Time (min)
C
vesicle
NS5B
buffer exchange
cIRES RNA
nucleoside triphosphates (NTPs)
Δ Normalize Frequency (Hz)
Time (min)
D
vesicle
NS5B
NS3
buffer exchange
cIRES RNA
nucleoside triphosphates (NTPs)
Δ Normalize Frequency (Hz)
Time (min)
E
vesicle
NS5B
buffer exchange
NS5A
buffer exchange
cIRES RNA
nucleoside triphosphates (NTPs)
lag time
Δ Normalize Frequency (Hz)
Time (min)
F
vesicle
NS5B
buffer exchange
cIRES RNA
NS5A
nucleoside triphosphates (NTPs)
lag time
Δ Normalize Frequency (Hz)
Time (min)
G
vesicle
NS5B
buffer exchange
cIRES RNA
nucleoside triphosphates (NTPs)
3′-dCTP
Δ Normalize Frequency (Hz)
Time (min)

Supporting Figure 8. No decline in resonance frequency is observed when fewer than all four native NTP species are added. RNA-dependent, RNA polymerase (RdRp) activity of the membrane-associated HCV replicase complex was assayed as in Supporting Figure 7C, except that only the indicated two (**A**), or three (**B**) NTP species were added.

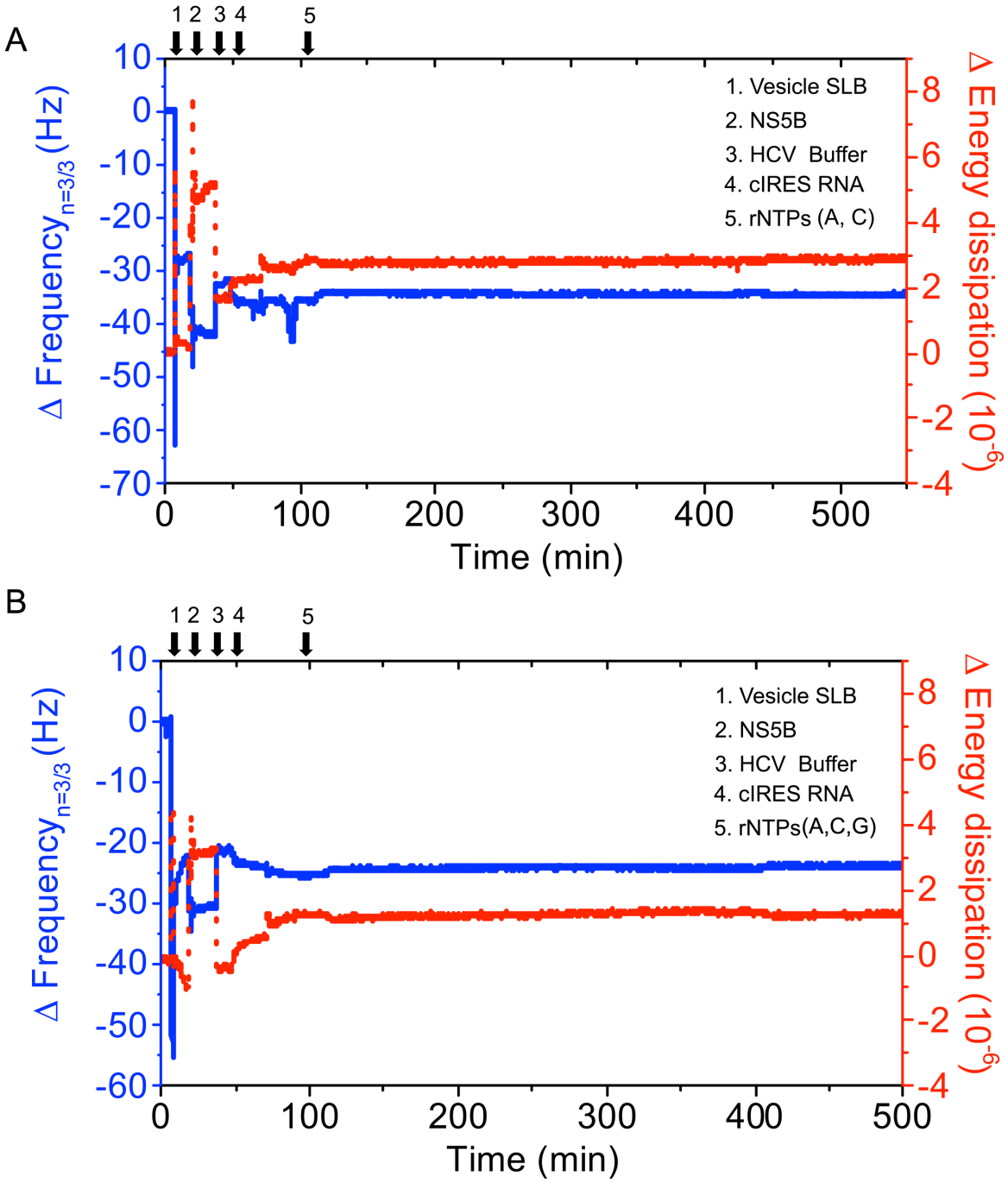

Supporting Figure 9. NS5AΔ32 Directly Binds to NS5B-FL. A) NS5A-FL protein binds to the SLB platform. **B)** NS5AΔ32 protein does not bind to the SLB platform. **C)** In the absence of cIRES RNA, NS5AΔ32 can still bind to the SLB platform, but only via binding to membrane-associated NS5B-FL.

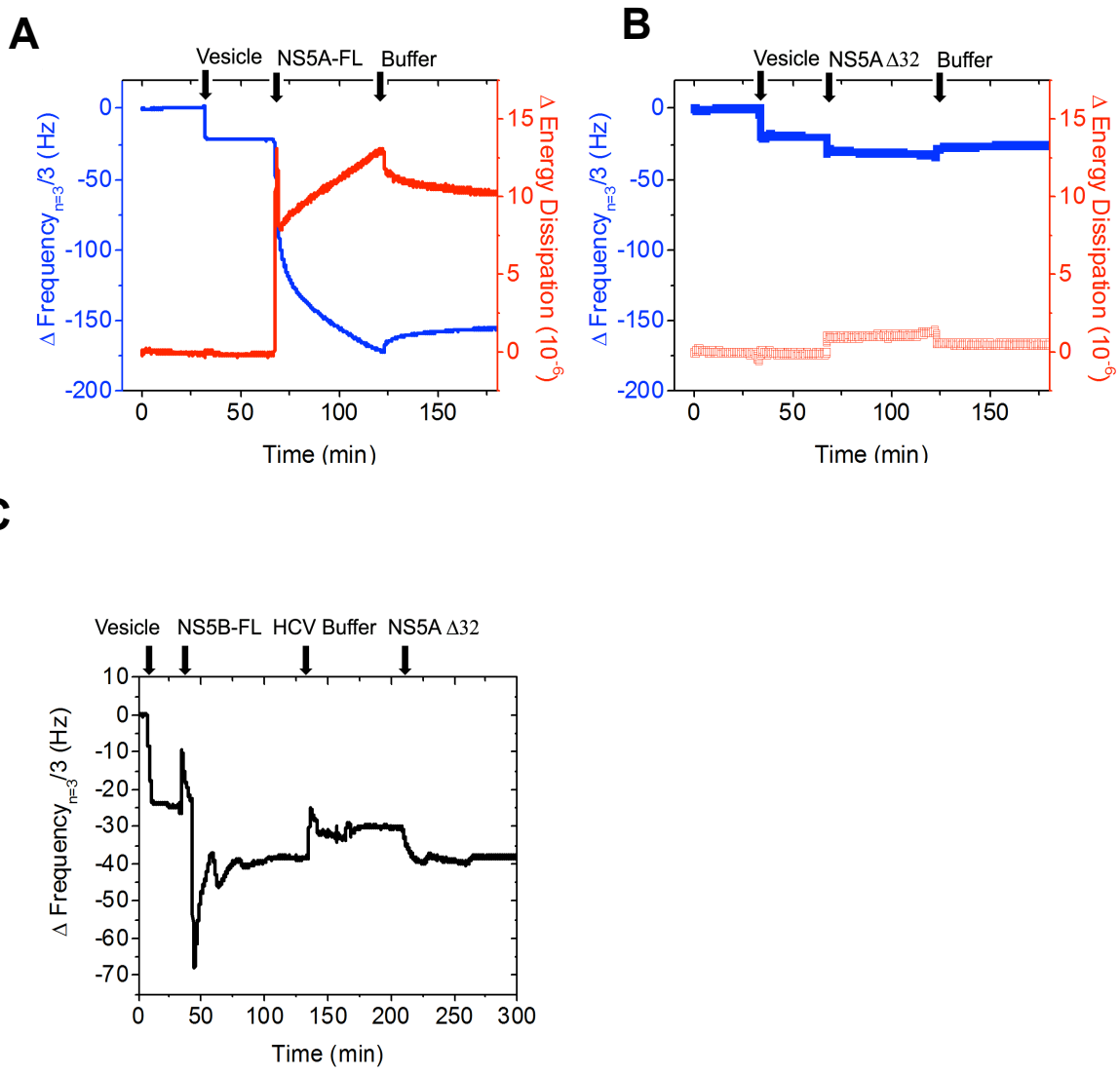

Supporting Figure 10. Northern blot analysis of QCM products. RNA synthesized from NS5B (NS5B-FL + cIRES RNA) or NS5B and NS5A (NS5B-FL + NS5AΔ32 + cIRES RNA), as in Supporting Figure 7C and E, respectively, was extracted using Trizol at the end of the QCM experiments and analyzed via Northern blot. Template RNA alone was run on the same gel. Positive controls (PC) of 2 different lengths (247 and 349 nts) corresponding to nucleotides 1 – 247 or 1 – 349 of the positive strand were included. Data are representative of 2 independently performed experiments.

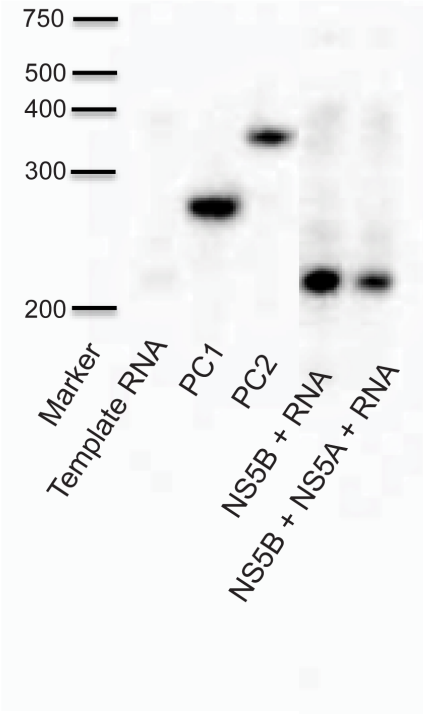

Supporting Figure 11. Chemical structures of non-nucleoside HCV NS5B inhibitors HCV-796 and VX-222.

HCV NS5B non-nucleoside inhibitor HCV-796:

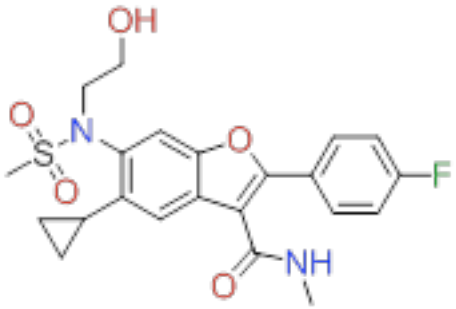

HCV NS5B non-nucleoside inhibitor VX-222:

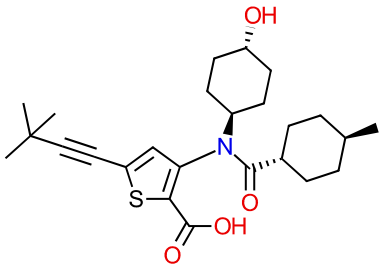

Supporting Table 1. Summary of Kinetic Values.

Protein	V_{max} [(1)] pmol.min^{-1}.cm^{-2}	[NS5B-FL] [(1)] pmol.cm^{-2}	V_{max} [(2)] pmol.min^{-1}	[NS5B] [(2)] pmol	k_{cat} min^{-1}	k_{cat} Fold shift
NS5B-FL	1.3 ± 0.1	9.9	N/A	N/A	0.13 ± 0.10	
NS5B-Δ21	N/A	N/A	0.10 ± 0.03	1	0.10 ± 0.03	0.8
NS5B-FL +NS3-FL	1.1 ± 0.3	9.3	N/A	N/A	0.12 ± 0.03	0.9
NS5B-FL +NS5A-Δ32	5.7 ± 2.1	6.7	N/A	N/A	0.83 ± 0.33	6.4

(1) On the SLB platform

(2) In solution

Supporting Table 2. QCM-D Measurement Data of Immobilized NS5B-FL Protein and Enzyme Kinetics. A) NS5B-FL. **B)** NS5B-FL + NS3-FL. **C)** NS5B-FL + NS5A-Δ32.

A) NS5B-FL

	Protein Immobilization			Enzyme Kinetics				
Run	NS5B-FL (Hz)	NS5B-FL[(1)] ($ng.cm^{-2}$)	NS5B-FL[(2)] ($pmol.cm^{-2}$)	NTP (Hz)	Time (min)	Vmax[(1)] ($ng.cm^{-2}.min^{-1}$)	Vmax[(3)] ($pmol.cm^{-2}.min^{-1}$)	k_{cat} (min^{-1})
1	33.4	591.2	9.0	9.7	360	0.48	1.4	0.16
2	41.3	731.0	11.1	8.4	360	0.41	1.2	0.11
3	35.9	636.0	9.7	8.7	360	0.43	1.3	0.13
4	36.0	637.0	9.7	9.6	360	0.47	1.4	0.14
Mean	36.7	648.8	9.9	9.1		0.45	1.3	0.13

B) NS5B-FL + NS3-FL

	Protein Immobilization			Enzyme Kinetics				
Run	NS5B-FL (Hz)	NS5B-FL[(1)] ($ng.cm^{-2}$)	NS5B-FL[(2)] ($pmol.cm^{-2}$)	NTP (Hz)	Time (min)	Vmax[(1)] ($ng.cm^{-2}.min^{-1}$)	Vmax[(3)] ($pmol.cm^{-2}.min^{-1}$)	k_{cat} (min^{-1})
1	32.3	571.5	8.7	5.9	360	0.29	0.9	0.10
2	36.6	647.7	9.9	9.3	360	0.46	1.3	0.14
Mean	34.4	609.6	9.3	7.6		0.37	1.1	0.12

C) NS5B-FL + NS5A-Δ32

	Protein Immobilization			Enzyme Kinetics				
Run	NS5B-FL (Hz)	NS5B-FL[(1)] ($ng.cm^{-2}$)	NS5B-FL[(2)] ($pmol.cm^{-2}$)	NTP (Hz)	time (min)	Vmax[(1)] ($ng.cm^{-2}.min^{-1}$)	Vmax[(3)] ($pmol.cm^{-2}.min^{-1}$)	k_{cat} (min^{-1})
1	25.5	451.4	6.9	18.8	140	2.38	7.0	1.02
2	22.9	404.6	6.2	4.8	90	0.94	2.8	0.45
3	26.7	471.7	7.2	19.4	139	2.47	7.3	1.01
Mean	25.0	442.6	6.7	14.3		1.93	5.7	0.83

(1) Frequency-to-mass conversion factor: 17.7 $Hz \cdot ng^{-1} \cdot cm^2$

(2) $MW^{NS5B\text{-}FL}$=65782 $g \cdot mol^{-1}$

(3) MW^{NMP} substrate = 340 $g \cdot mol^{-1}$

References

1. Lesburg, C. A.; Cable, M. B.; Ferrari, E.; Hong, Z.; Mannarino, A. F.; Weber, P. C., Crystal structure of the RNA-dependent RNA polymerase from hepatitis C virus reveals a fully encircled active site. *Nat. Struct. Mol. Biol.* **1999,** *6*, 937-943.

2. Cho, N. J.; Frank, C. W.; Kasemo, B.; Hook, F., Quartz crystal microbalance with dissipation monitoring of supported lipid bilayers on various substrates. *Nat. Protoc.* **2010,** *5*, 1096-1106.

3. Cho, N. J.; Frank, C. W., Fabrication of a planar zwitterionic lipid bilayer on titanium oxide. *Langmuir* **2010,** *26*, 15706-15710.

4. Cho, N. J.; Jackman, J. A.; Liu, M.; Frank, C. W., pH-driven assembly of various supported lipid platforms: A comparative study on silicon oxide and titanium oxide. *Langmuir* **2011,** *27*, 3739-3748.

5. Jackman, J. A.; Cho, N. J.; Duran, R. S.; Frank, C. W., Interfacial binding dynamics of bee venom phospholipase A_2 investigated by dynamic light scattering and quartz crystal microbalance. *Langmuir* **2010,** *26*, 4103-4112.

6. Reimhult, E.; Höök, F.; Kasemo, B., Vesicle adsorption on SiO_2 and TiO_2: Dependence on vesicle size. *J. Chem. Phys.* **2002,** *117*, 7401-7404.

7. Reimhult, E.; Höök, F.; Kasemo, B., Intact vesicle adsorption and supported biomembrane formation from vesicles in solution: Influence of surface chemistry, vesicle size, temperature, and osmotic pressure. *Langmuir* **2003,** *19*, 1681-1691.

8. McCubbin, G. A.; Praporski, S.; Piantavigna, S.; Knappe, D.; Hoffmann, R.; Bowie, J. H.; Separovic, F.; Martin, L. L., QCM-D fingerprinting of membrane-active peptides. *Eur Biophys. J.* **2011,** *40*, 437-446.